# LONGITUDINAL HYDRAULIC RESISTANCE PARAMETERS OF CRYOCOOLER AND STIRLING REGENERATORS IN STEADY FLOW

Cite as: AIP Conference Proceedings **985**, 728 (2008); https://doi.org/10.1063/1.2908664
Published Online: 27 March 2008

**W. M. Clearman, S. M. Ghiaasiaan, J. S. Cha, C. S. Kirkconnell, and P. V. Desai**

AIP Conference Proceedings **985**, 728 (2008); https://doi.org/10.1063/1.2908664 

# LONGITUDINAL HYDRAULIC RESISTANCE PARAMETERS OF CRYOCOOLER AND STIRLING REGENERATORS IN STEADY FLOW

W. M. Clearman, S. M. Ghiaasiaan, J. S. Cha, C. S. Kirkconnell[1], P. V. Desai

G.W. Woodruff School of Mechanical Engineering
Georgia Institute of Technology, Atlanta, Ga., U.S.A.

[1]Raytheon Space and Airborne Systems (SAS)
El Segundo, CA 90245-0902, U.S.A.

## ABSTRACT

The results of an ongoing research program aimed at the measurement and correlation of anisotropic hydrodynamic parameters of widely-used cryocooler regenerator fillers are presented. The hydrodynamic parameters associated with steady, longitudinal flow are addressed in this paper. An experimental apparatus consisting of a cylindrical test section packed with regenerator fillers is used for the measurement of axial permeability and Forchheimer coefficients, with pure helium as the working fluid. The regenerator fillers that are tested include stainless steel 325 and 400-mesh screens with 69.69% porosity, stainless steel 400-mesh sintered mesh filler with 61.65% porosity, stainless steel foam metal with 55.47% porosity, and micro machined nickel disks with 26.8% porosity. The test section is subjected to a steady flow of helium at one end, and is open to the atmosphere at the other end. The instrumentation includes pressure transducers and a high-precision flow meter. For each filler material, the pressures at inlet to the regenerator are measured under steady flow conditions over a wide range of flow rates and a CFD assisted methodology is then used for the analysis and interpretation of the measured data. The viscous and inertial resistance parameter values, and the corresponding permeability and inertial coefficients, obtained using CFD are then compared with the corresponding values that are separately measured under steady-periodic flow conditions.

**KEYWORDS:** Pulse tube, steady flow, permeability, inertial coefficient, axial flow, porous media

CP985, *Advances in Cryogenic Engineering: Transactions of the Cryogenic Engineering Conference—CEC, Vol. 53,* edited by J. G. Weisend II

## INTRODUCTION

Improving the performance of the various types of cryocoolers is of great interest. For pulse tube refrigerators, there are several sources of irreversibility [1] but the regenerator is typically the largest source of loss in cryocoolers [2]. Axial heat conduction, thermal saturation, and frictional losses all cause irreversibility. However, it is very difficult to accurately predict the impact of the solid-fluid interactions within the porous media for periodic flow. To simplify the analysis of these periodic systems, isotropic hydrodynamic parameters associated with steady flow have often been used [3]. It has recently been shown that CFD tools can simulate the entire cryocooler devices under steady and steady-periodic conditions [11, 12, 13]. However, the accuracy of these CFD predictions depend strongly on the accuracy of the closure relations they use.

In this investigation measured pressure drops across cylindrical test sections containing various regenerator filler structures that are subject to a steady flow of helium are reported. These data were used as boundary conditions for CFD simulations of the test section. Through an iterative process, the axial viscous resistance, $D$, and the inertial resistance, $C$, were adjusted to match simulated results to the experimental data. Using these results, the permeability and Forchheimer's coefficients were then calculated.

## TEST APPARATUS

The test apparatus (Figure 1) includes a helium tank, two high frequency Paine Electronics pressure transducers (Series 210-10), a Sierra Instruments hot plate mass flow meter (Model 826 Toptrak), and test section containing the regenerator fillers of interest. Details of the 3-piece aluminum test section are displayed in Figure 2. The regenerator test sections is a slight variation of the design used by Cha [4]. It is made of aluminum 6061 and consists of the regenerator housing containing a 5/16" (0.79 cm) diameter by 1.5" (3.81 cm) length open volume for the test samples as well as two end pieces to hold the regenerator material in place. A larger regenerator housing 0.59" (1.499 cm) in diameter and 1.236" (3.139 cm) in length was used for the micro machined disk samples. The helium tank contains research grade *He* with a nominal purity of 99.999%. Experimental pressure drop data were recorded for the five matrix samples for flow rates between 0 g/s to 1.5 g/s. The porous structures tested included 325 mesh and 400 mesh stainless steel screens at 69.69% and 69.68% porosity, respectively, sintered 400 mesh stainless steel screens at 61.65% porosity, stainless steel foam metal at 55.47% porosity, and stacked, micro machined nickel disks at 26.8% porosity. The latter regenerator filler was made of disks that were provided by International Mezzo Technologies, Inc. Baton Rouges, Louisiana). The disks had holes with diameter in the range 36~40 $\mu$m, and could be stacked such that the holes would get completely aligned.

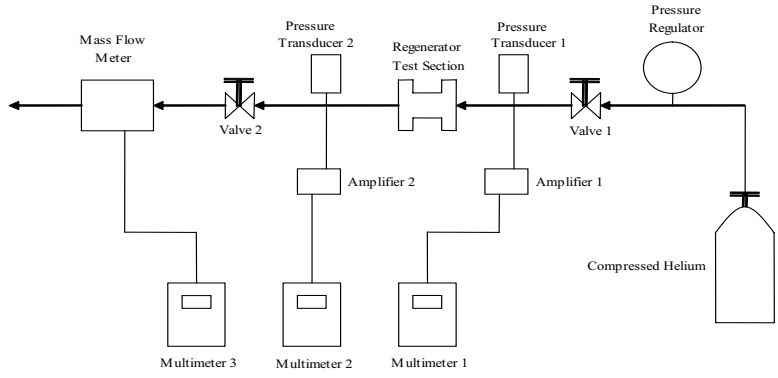


**FIGURE 1.** Axial pressure drop test apparatus.

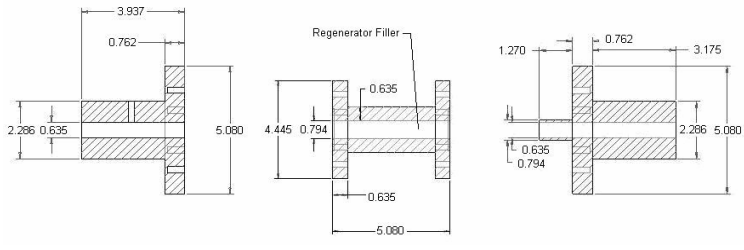


**FIGURE 2.** Detailed test section (dimensions in cm).

## RESULTS OF EXPERIMENTS

Multiple pressure drop tests were conducted for each of the five porous structures of interest. Figures 3 and 4 show the steady flow axial pressure drop as a function of the measured mass flow rate.

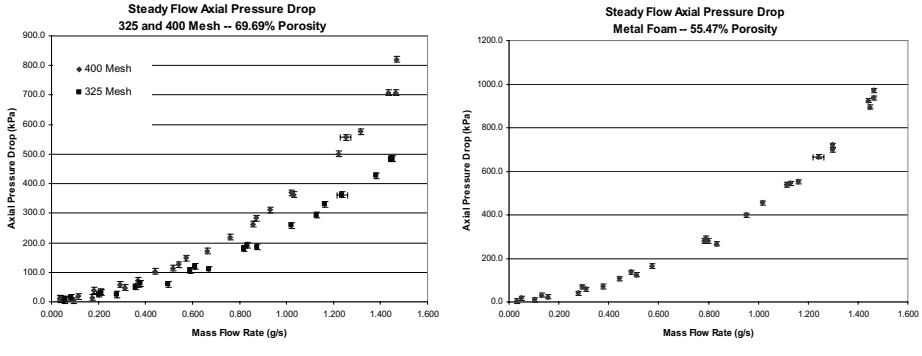


(a) (b)

**FIGURE 3.** Steady flow axial pressure drop data for (a) 325 mesh and 400 mesh (b) metal foam

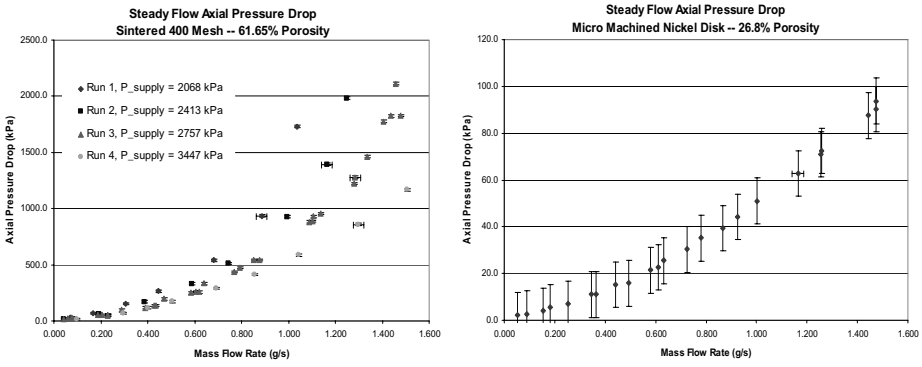


(a) (b)

**FIGURE 4.** Steady flow axial pressure drop data metal foam (a) sintered 400 mesh (b) machined nickel disks.

For the sintered 400 mesh sample, the 300 psia (2068 kPa) supply pressure, or regulator pressure, was insufficient to achieve a gas flow of 1.5 gm/s. Therefore, four series of runs representing supply pressures covering the range 2068 kPa to 3447 kPa were performed for this filler (Figure 4a).

## CFD MODEL

Using Fluent [14], the entire regenerator test section and its vicinity were modeled and used along with the empirically measured boundary conditions (inlet pressure and mass flow rate) and user defined values of the relevant hydrodynamic parameters. The simulated outlet pressure, and thus the simulated pressure drop across the porous medium could then be adjusted to match the actual pressure drop by varying the assigned values of the viscous and inertial resistances.

For the open region of the test section model, Fluent solves the following continuum based mass, momentum, and energy conservation equations:

$$\frac{\partial \rho}{\partial t} + \nabla \cdot (\rho \vec{v}) = 0 \tag{1}$$

$$\frac{\partial}{\partial t}(\rho \vec{v}) + \nabla \cdot (\rho \vec{v} \vec{v}) = -\nabla P + \nabla \cdot \bar{\bar{\tau}} + \rho \vec{g} + \vec{F} \tag{2}$$

$$\frac{\partial}{\partial t}(\rho E) + \nabla \cdot (\vec{v}(\rho E + P)) = -\nabla \cdot \left( \sum_j h_j J_j \right) + S_h \tag{3}$$

where

$$\bar{\bar{\tau}} = \mu \left[ \left( \nabla \vec{v} + \nabla \vec{v}^T \right) - \frac{2}{3} \nabla \cdot \vec{v} \bar{\bar{I}} \right] \tag{4}$$

For the porous regions of the model, the following volume-average governing equations are solved assuming isotropic porosity, $\varepsilon$:

$$\frac{\partial(\varepsilon\rho)}{\partial t} + \nabla\cdot(\varepsilon\rho\vec{v}) = 0 \tag{5}$$

$$\frac{\partial(\varepsilon\rho\vec{v})}{\partial t} + \nabla\cdot(\varepsilon\rho\vec{v}\vec{v}) = -\varepsilon\nabla P + \nabla\cdot(\varepsilon\vec{\tau}) + \varepsilon\vec{g} + \vec{F} \tag{6}$$

$$\frac{\partial}{\partial t}\left(\varepsilon\rho_f E_f + (1-\varepsilon)\rho_s E_s\right) + \nabla\cdot\left(\vec{v}\left(\rho_f E_f + P\right)\right) = \nabla\cdot\left[k_{eff}\nabla T - \left(\sum_i h_i J_i\right) + \left(\bar{\bar{\tau}}\cdot\vec{v}\right)\right] + S_f^h \tag{7}$$

where the external body force term of the momentum equation is modeled as

$$F_i = -\left(\sum_{j=1}^{3} D_{ij}\mu v_j + \sum_{j=1}^{3} C_{ij}\frac{1}{2}\rho v_{mag} v_j\right) \tag{8}$$

The regenerator is axi-symmetric, and its axial direction is a principle direction for the porous medium. Therefore, when flow in the axial direction is considered the coefficients in the last two terms of Eq. (8) can be represented as Darcy permeability, $K_x$ and Forchheimer's inertial coefficient, $c_{f,x}$, by the following relationship [7]:

$$K_x = \frac{\varepsilon^2}{D_x} \qquad\qquad c_{f,x} = \frac{C_x\sqrt{K_x}}{2\varepsilon^3} \tag{9}$$

## RESULTS AND DISCUSSION

Figure 5 shows the CFD model nodalization scheme consisting of 2200 total nodes that was used for all the filler structures except for the perforated disks. For the perforated disks, the dimensions of the test section were slightly different and the total number of nodes was 3600.

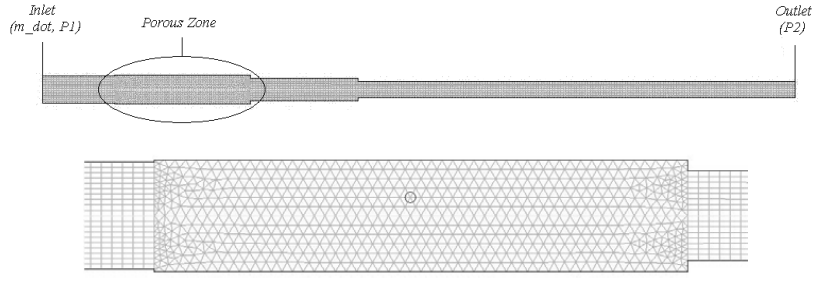


**FIGURE 5.** Nodalization of test section and vicinity.

Assuming steady, 1-D flow of helium, and neglecting axial body forces and enthalpy sources, the pressure drop and mass flow data determined from experimentation could be used along with user defined values of $D$ and $C$ to close and numerically solve the governing system of equations. After iteratively adjusting the magnitudes of the hydrodynamic parameters to reduce the average percent difference between simulated and experimental pressure drop, the values of the viscous and inertial resistances resulting in the most accurate simulations were recorded in Table 1.

These values of $D$ and $C$ can now be compared directly to the periodic hydrodynamic parameters determined by Cha [4] for identical porous structures. Data indicates that there can be a difference between the steady and periodic flow viscous resistance of as much as 42.6% while there can be a difference between the steady and periodic flow inertial resistance of as much as 57.7%. Using steady flow hydrodynamic parameters to predict behavior of periodic flow through porous media can thus lead to substantial inaccuracies. This data can also be compared with the directional radial hydrodynamic parameters [5]. For the stacked 325 mesh screens at 69% porosity, the axial viscous resistance was 350% higher and the inertial resistance was 50% lower than the same parameters in the radial direction.

**TABLE 1.** Steady flow axial hydrodynamic parameters [7].

| Regenerator Material | Porosity (%) | D (1/m^2) | C (1/m) | K (m^2) | $c_f$ ( - ) |
|---|---|---|---|---|---|
| 400 Mesh | 69.69 | 2.77E+10 | 73000 | 1.753E-11 | 0.452 |
| 325 Mesh | 69.69 | 2.35E+10 | 47000 | 2.067E-11 | 0.316 |
| 400 Sintered (2068 kPa) | 61.65 | 5.898E+10 | 259768 | 6.444E-12 | 1.407 |
| 400 Sintered (2413 kPa) | 61.65 | 5.813E+10 | 250104 | 6.538E-12 | 1.365 |
| 400 Sintered (2757 kPa) | 61.65 | 5.682E+10 | 235594 | 6.689E-12 | 1.300 |
| 400 Sintered (3447 kPa) | 61.65 | 5.496E+10 | 215834 | 6.916E-12 | 1.211 |
| Metal Foam | 55.47 | 2.65E+10 | 99000 | 1.161E-11 | 0.988 |
| Machined Disk | 26.80 | 2.30E+10 | 115000 | 3.123E-12 | 5.279 |

All the experimental measurements were performed with a supply pressure (i.e., pressure upstream Valve 1 in Figure 1) of 2068 kPa, except for the sintered 400 mesh filler. For this filler, a series of experiments were performed with back pressures of 2068 kPa, 2413 kPa, 2757 kPa, and 3447 kPa (300, 350, 400, and 500 psia), in order to examine the effect of pressure on the hydrodynamic parameters. Figure 6a shows that using the hydrodynamic parameters associated with a supply pressure of $P_{supply}$ = 2757 kPa to simulate flow at other supply pressures leads to systematic discrepancies between data and CFD predictions. To correct for the effect of pressure on the hydrodynamic parameters, the following correlation was proposed:

$$D = D_0 \left( \frac{P_{av}}{P_{cr}} \right)^{n_1} \tag{10}$$

$$C = C_0 \left( \frac{P_{av}}{P_{cr}} \right)^{n_2} \tag{11}$$

where $P_{av}$ is the average pressure in the porous test section, and $P_{cr}$ is the fluid critical pressure. The constants $D_0$ = 6.650E+10 $m^{-2}$, $n_1$ = -0.08, $C_0$ = 356000 $m^{-1}$, and $n_2$ = -0.21 were iteratively determined by seeking the minimum average error between the adjusted hydrodynamic parameters as calculated by Eq. 10 and Eq. 11 and the actual parameters determined through simulations fit to the experimental data for each individual supply pressure.

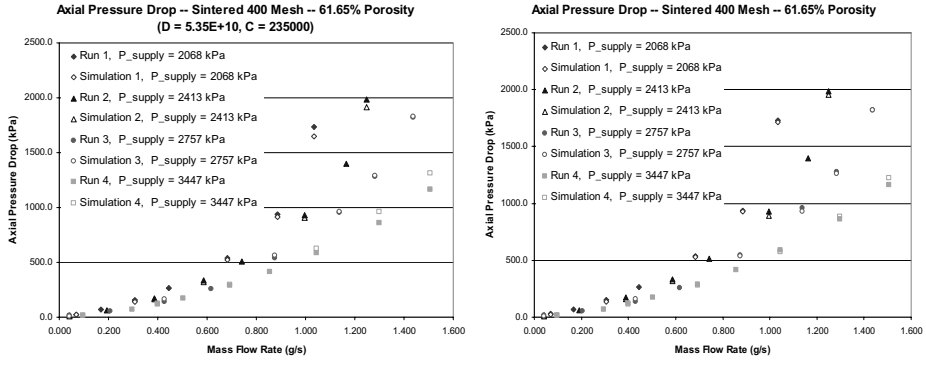


(a) (b)

**FIGURE 6**. Simulation vs. experimental pressure drop using (a) constant hydrodynamic parameters and (b) using pressure dependant hydrodynamic parameters.

## CONCLUSIONS

In this investigation, experiments were performed for the measurement and correlation of axial viscous and inertial resistance parameters associated with some common cryocooler regenerator structures. The data analysis was performed using a CFD-assisted method. The structures studied included stacked 325 mesh screens, stacked 400 mesh screens, sintered 400 mesh screens, metal foam, and stacked micro machined disks. The steady flow and periodic flow viscous and inertial resistances were compared for identical porous structures, and were found to be different. Thus, it was concluded that the behavior of periodic flow within the porous cryocooler regenerator cannot be accurately predicted based on steady flow hydrodynamic parameters. Likewise, the anisotropic parameters for a single porous sample were reported. The experimental data showed that the viscous and inertial resistances, and thus the permeability and Forchheimer coefficient, are functions of pressure. The dependence of both parameters on pressure was empirically correlated for the sintered 400 mesh structure.

## ACKNOWLEDGEMENTS

This research is supported by Raytheon Company. We would like to thank Dr. Carl S. Kirkconnell and Jeesung Cha for technical assistance.

## NOMENCLATURE

| | |
|---|---|
| $A$ | area of flow tube ($m^2$) |
| $c_f$ | Forchheimer coefficient |
| $C_{ij}$ | inertial resistance matrix ($m^{-1}$) |
| $D_{ij}$ | viscous resistance matrix ($m^{-2}$) |
| $E$ | total specific energy (kJ/kg) |
| $F$ | external body force vector ($N/m^3$) |
| $\vec{g}$ | gravitational acceleration ($m/s^2$) |
| $\bar{\bar{I}}$ | unit tensor |
| $J_i$ | diffusion flux of species $i$ ($kg/m^2s$) |
| $k$ | thermal conductivity (W/m-K) |
| $K$ | permeability ($m^2$) |
| $\dot{m}$ | mass flow rate of working fluid (kg/s or g/s) |
| $P$ | fluid pressure (Pa) |
| $S^h$ | enthalpy source ($W/m^3$) |
| $T$ | temperature (K) |
| $T_\infty$ | bulk fluid temperature (K) |
| $t$ | time (s) |
| $\vec{v}$ | physical velocity vector (m/s) |
| $\dot{V}$ | volumetric flow rate ($m^3/s$) |
| $x$ | axial coordinate (m) |

*Greek letters*

| | |
|---|---|
| $\varepsilon$ | porosity |
| $\mu$ | fluid dynamic viscosity ($N\text{-}s/m^3$) |
| $\rho$ | density ($kg/m^3$) |
| $\bar{\bar{\tau}}$ | viscous stress tensor (Pa) |

*Subscripts and Symbols*

| | |
|---|---|
| *av* | average |
| *cr* | critical |
| *eff* | effective |
| *f* | fluid |
| *s* | solid |
| $\nabla$ | Del operator ($m^{-1}$) |

## REFERENCES


1 Gifford, W.E. , Longsworth, R.C., "Pulse Tube Refrigeration Progress." Advances in Cryogenic Engineering, Vol. 10. Plenum Press, New York, 1964. pp. 69-79.

2 Radebaugh, R., Lewis, M., Luo, E., Pfotenhauer, J.M., Nellis, G.F., Schunk, L.A., "Inertance Tube Optimization for Pulse Tube Cryocoolers." Advances in Cryogenic Engineering: Transactions of the Cryogenic Engineering Conference, Vol. 51, 2006. pp. 59-67.

3 Harvey, J.P., "Oscillatory Compressible Flow and Heat Transfer in Porous Media – Application to Cryocooler Regenerators." PHD Dissertation, Georgia Institute of Technology, Atlanta, GA. 2003.

4 Cha, J.S., "Measurement And Correlation Of Anisotropic Hydrodynamic Parameters In Porous Media Under Steady And Oscillating Flow: Application To Cryocooler Regenerator." PHD Dissertation, Georgia Institute of Technology, Atlanta, GA. 2007.

5 Cha, J.S., Ghiaasiaan, S.M., Desai, P.V., "Measurement of Anisotropic Hydrodynamic Parameters of Pulse Tube or Stirling Regenerators." Advances in Cryogenic Engineering: Transactions of the Cryogenic Engineering Conference, Vol. 51, 2006. pp. 1911-1918.

6 Vafai, K., Editor. "Handbook of Porous Media." 2nd Edition. Taylor and Francis Group, 2005.

7 Clearman, W.M., "Measurement and Correlation of Directional Permeability and Forchheimer's Inertial Coefficient of Micro Porous Structures Used in Pulse-Tube Cryocoolers," Master's Thesis, Georgia Institute of Technology, Atlanta, GA. 2007.

8 Cha, J.S., "CFD Simulation of Multi-Dimensional Effects in Inertance Tube Pulse Tube Cryocoolers," Master's Thesis, Georgia Institute of Technology, Atlanta, GA. 2004.

9 Nam, K., Jeong, S., "Measurement of Cryogenic Regenerator Characteristics under Oscillating Flow and Pulsating Pressure." Cryogenics 43, Elsevier, 2003. pp. 575-581.

10 Jeong, Nam, Jung, "Regenerator Characterization under Oscillating Flow and Pulsating Pressure." Cryocoolers 12, Kluwer Academic, New York, 2003. pp. 531.

11 Hozumi, Y., and Shiraishi, M., "Simulation of Thermodynamics Aspects About Pulse Tube Refrigerator," Proc. Int. Cryo. Eng. Conf., Sept 2003, pp. 1500-1507.

12 Flakes, B., and Razani, A., "Modeling Pulse Tube Cryocoolers with CFD," Proc. Int. Cryo. Eng. Conf., September 2003, pp. 1493-1499.

13 Cha, J.S., Ghiaasiaan, S.M., Desai, P.V., Harvey, J.P., and Kirkconnel, C.S., "Multi-dimensional Flow Effects in Pulse Tube Refrigerators," Cryogenics, Vol. 46 (2006), pp. 658-665.

14 "Fluent 6.2 User's Guide." January, 2005. Chapters 7 & 9.